frontiers in Microbiology

ORIGINAL RESEARCH
published: 09 February 2021
doi: 10.3389/fmicb.2020.621463

A Hyper-Attenuated Variant of Rift Valley Fever Virus Generated by a Mutagenic Drug (Favipiravir) Unveils Potential Virulence Markers

Belén Borrego and Alejandro Brun*

Centro de Investigación en Sanidad Animal (CISA), Instituto Nacional de Investigación y Tecnología Agraria y Alimentaria (INIA), Madrid, Spain

Rift Valley fever virus (RVFV) is a mosquito-borne bunyavirus that causes Rift Valley fever (RVF), a zoonotic disease of wild and domestic ruminants, causing serious economic losses and a threat to human health that could be controlled by vaccination. Though RVF vaccines are available for livestock, no RVF vaccines have been licensed for veterinary use in non-endemic countries nor for human populations in RVF risk areas. In a recent work, we showed that favipiravir, a promising drug with antiviral activity against a number of RNA viruses, led to the extinction of RVFV from infected cell cultures. Nevertheless, certain drug concentrations allowed the recovery of a virus variant showing increased resistance to favipiravir. In this work, we characterized this novel resistant variant both at genomic and phenotypic level *in vitro* and *in vivo*. Interestingly, the resistant virus displayed reduced growth rates in C6/36 insect cells but not in mammalian cell lines, and was highly attenuated but still immunogenic *in vivo*. Some amino acid substitutions were identified in the viral RNA-dependent RNA-polymerase (RdRp) gene and in the virus encoded type I-interferon (IFN-I) antagonist NSs gene, in catalytic core motifs and nuclear localization associated positions, respectively. These data may help to characterize novel potential virulence markers, offering additional strategies for further safety improvements of RVF live attenuated vaccine candidates.

Keywords: Rift Valley fever virus, favipiravir, live attenuated vaccines, virulence markers, mutagenesis

SIGNIFICANCE STATEMENT

Live attenuated virus vaccines usually provide long lasting immune responses upon administration. These vaccines are not recommended for use in immune compromised hosts, due to the presence of uncontrolled residual virulence. Cell culture virus propagation in the presence of mutagenic drugs often results in weakened virus lacking virulence as well as limited spreading capabilities. Here, we have characterized a mutagen-induced RVFV variant (40F-p8) that is not virulent in an extremely sensitive mouse strain lacking antiviral response. The observed lack of virulence correlates with the presence of specific mutations along key residues in the viral genome, unveiling potential virulence determinants. Thus, 40F-p8 constitutes the basis for a novel RVFV vaccine strain with additional safety features.

OPEN ACCESS

Edited by:
Helene Dutartre,
UMR5308 Centre International de Recherche en Infectiologie (CIRI), France

Reviewed by:
Alexander Freiberg,
University of Texas Medical Branch at Galveston, United States
Tetsuro Ikegami,
University of Texas Medical Branch at Galveston, United States

****Correspondence:***
Alejandro Brun
brun@inia.es

Specialty section:
This article was submitted to Virology, a section of the journal Frontiers in Microbiology

Received: *28 October 2020*
Accepted: *21 December 2020*
Published: *09 February 2021*

Citation:
Borrego B and Brun A (2021) A Hyper-Attenuated Variant of Rift Valley Fever Virus Generated by a Mutagenic Drug (Favipiravir) Unveils Potential Virulence Markers. Front. Microbiol. 11:621463. doi: 10.3389/fmicb.2020.621463

INTRODUCTION

Rift Valley fever virus (RVFV), a mosquito-borne bunyavirus belonging to the genus Phlebovirus in the *Phenuiviridae* family, causes an important disease in domesticated ruminants often transmitted to humans mainly through mosquito bites after epizootic outbreaks. Rift Valley fever (RVF) is currently confined to the African continent and Southern parts of the Arabian Peninsula and Indian Ocean islands but its potential for spreading to other geographical areas, particularly linked to climatic change and globalization, has been widely remarked (Rolin et al., 2013). In 2017, the World Health Organization ranked RVFV among the ten "most dangerous pathogens most likely to cause wide epidemics in the near future, requiring urgent attention" (http://www.who.int/blueprint/priority-diseases/en/). Currently, there is no available treatment or fully licensed RVF vaccines for use in non-endemic areas; consequently, developing of safer and effective control strategies intended also for human use is an active field of research.

The RVFV virion structure is formed by a lipidic envelope with two tightly packed membrane glycoproteins (Gn and Gc) arranged in an icosahedral lattice protecting an internal nucleocapsid composed by the viral nucleoprotein (N) and a RNA dependent RNA polymerase (RdRp) bound to the viral RNA. The genome of RVFV is composed of three ssRNA segments of different size (*L*arge, *M*edium, and *S*mall) with negative (L and M) or ambisense (S) polarity (Boshra et al., 2011). While the L segment codes for the viral RdRp the M segment codes both glycoproteins, a 78kDa protein found only in virions produced in insect cells (Weingartl et al., 2014) and a non-structural protein that can be found in two different isoforms of 13kDa (NSm') or 14kDa (NSm) due to different use of in-frame start codons (Kreher et al., 2014). Finally, the the S segment encodes the viral nucleoprotein and a non-structural 30kDa protein (NSs) considered the main virulence factor of the virus.

As many acute systemic viral infections, live-attenuated RVFV rapidly induce a long-lasting and broadly protective immunity after a single inoculation (Sabin and Blumberg, 1947; Poland et al., 1981). Therefore, vaccines based on attenuated virus remain as excellent candidates for a successful immunization program in the affected countries or as preventive control measure in countries with more elevated risk of disease introduction. For Rift Valley fever, live-attenuated vaccines have been generated either by random mutagenesis (Caplen et al., 1985) or, more recently, by rationale deletion of virulence-associated genes using reverse genetics (Bird et al., 2008). In both cases, critical attenuating mutations or virulence determinants were identified, adding more available knowledge for further safety improvements. However, the use of live attenuated vaccines in RVF endemic areas may still cause some safety concerns due to the possibility of genetic reassortment between genome segments of closely related virus strains (Sall et al., 1999). Although this phenomenon has been more often described for members of the orthobunyavirus genus (Briese et al., 2013) it is still considered as a potential drawback for live attenuated RVF vaccines. Additionally, although highly attenuated *in vivo,* these vaccines may retain some residual virulence, as shown upon experimental infection in immunocompromised lab animal models (Bouloy et al., 2001; Gommet et al., 2011) or in pregnant sheep when overdosed (Makoschey et al., 2016).

In a previous work, aimed to analyze the mutagenic effect of the nucleoside analog favipiravir on RVFV growth in *vitro,* we found that the propagation of the RVFV strain 56/74 in the presence of this drug led to virus extinction by a mechanism of lethal mutagenesis (Borrego et al., 2019). Unexpectedly, at a dose of 40 μM favipiravir, cytopathic effect (CPE) was detected in cell cultures after a lag phase (with no detectable CPE) of three consecutive blind passages. This finding was suggestive of incomplete or ineffective virus extinction leading to the selection of favipiravir-resistant variants. In this work, the virus recovered after eight serial passages in the presence of 40 μM favipiravir (namely 40F-p8) was selected for further genomic, phenotypic and immunogenic characterization. The 40F-p8 virus displayed reduced growth rates in insect cells and, most interestingly, a "hyper attenuated" phenotype *in vivo*, as shown by the lack of virulence in the highly susceptible A129 mice (IFNAR$^{-/-}$). These distinct features indicate that other virulence markers encoded in the RVFV genome remain to be characterized. Identification of these cryptic markers may help to strength the safety of live attenuated RVF vaccines.

RESULTS

Phenotypic Characterization of Mutagen Resistant RVFV 40F-p8 in Cell Culture

Firstly, we analyzed the kinetics and total virus yield of 40F-p8, the resistant virus recovered after eight serial passages in Vero cells in the presence of 40 μM favipiravir. The parental virus before (56/74) and after propagation along the same number of passages but in the absence of drug (56/74-p8) were included for comparison purposes. Growth was monitored in either interferon type-I responsive (HEK293) or non-responsive (Vero) cell lines. Since RVFV is an arbovirus, with mosquitoes playing an important role in the natural transmission cycle, infections were also carried out in *Ae.albopictus* clone C6/36 mosquito larvae derived cell line. Infections carried out in Vero cells showed growth curves similar for the three viruses (**Figure 1A**). Titration of supernatants collected at different times post infection in several independent experiments showed only slight differences among the three viruses recovered. While the growth pattern of the virus passaged eight times in the absence of drug showed no differences with the parental RVFV 56/74, the selected 40F-p8 virus displayed slightly faster growth, producing higher virus yields at 3-4 dpi that did not reach enough statistical significance (multiple *t*-test). No differences in growth kinetics were observed in HEK293 cells (**Figure 1B**), suggestive of a competent interferon antagonistic phenotype of 40F-p8 indistinguishable from both the parental strain 56/74 or the Vero cell passaged 56/74-p8.

Conversely, both viral growth and final yield in C6/36 mosquito cells were clearly reduced for the selected 40F-p8 virus

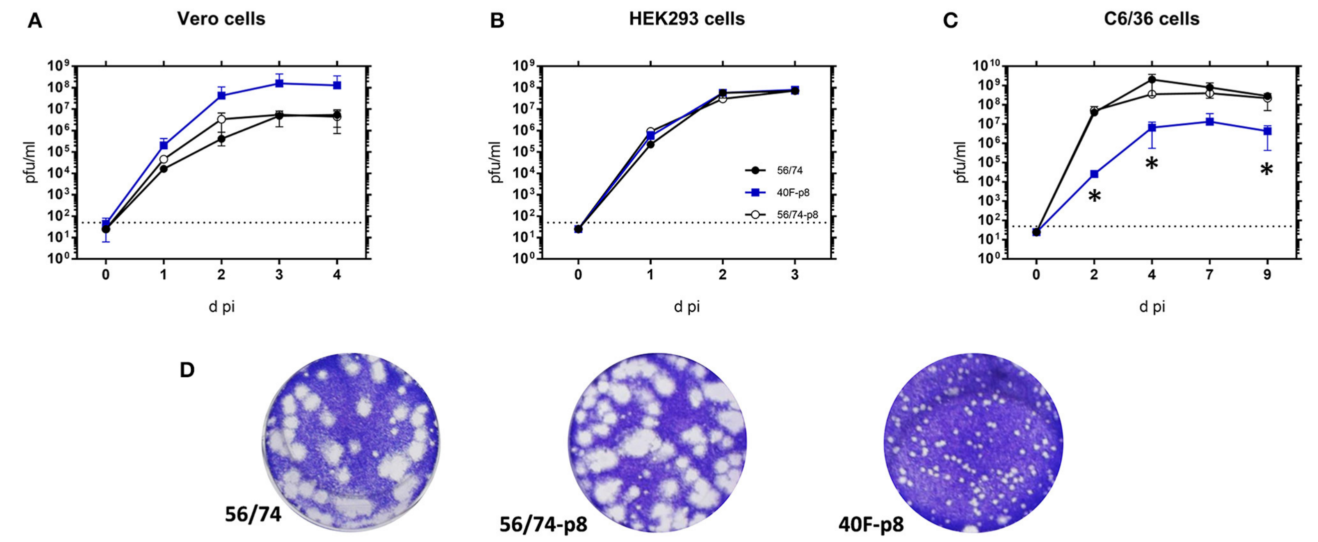

FIGURE 1 | Kinetics of growth in mammalian and insect cells. Vero cells **(A)** and HEK293 **(B)** were infected at a MOI of 0.01 while C6/36 mosquito cells **(C)** were infected with 0.005 pfu/cell. After 1 h of adsorption the inoculum was removed, cells were washed and fresh medium was added. Supernatants were collected at different times post infection (pi) and titrated on Vero cell monolayers Independent titrations were performed in duplicates in at least two independent experiments. Mean values ± SD are represented. Significance level was set to $^{*}P < 0.05$ (multiple t-test using the Holm–Sidak method, with alpha = 5.000%). Data shown correspond to one representative experiment. **(D)** Plaque phenotypes of the indicated viruses on Vero cell monolayers.

(**Figure 1C**). Since infected mosquito C6/36 cells remain viable for longer times in cell culture than Vero cells, the analysis could be extended up to 9 days. In insect cells, the growth of 40F-p8 was significantly delayed, with viral titers of 10^4 pfu/ml at day 2 pi, at least 3 log units lower than those rendered by the control viruses. Total virus yields at the latest points analyzed (7–9 days pi), although reaching a titer of 10^7 pfu/ml, were still below the one reached by the parental RVFV 56/74 ($>10^8$ pfu/ml). In contrast, no significant changes were found for 56/74-p8 with respect to the parental 56/74 virus.

Although the results obtained in Vero and HEK293 cells (**Figures 1A,B**) did not show statistically significant differences among the three viruses, the plaque phenotype of 40F-p8 differed substantially, rendering smaller plaques than those produced by either the parental virus or by 56/74-p8 grown in the absence of favipiravir (**Figure 1D**).

Analysis of the Infectivity of RVFV 40F-p8 in A129 Mice (IFNAR$^{-/-}$)

Previous works have shown that viruses displaying some resistance to mutagenic antivirals are attenuated *in vivo* (Coffey et al., 2011; Cheung et al., 2014). In fact, mutagen treatment has been often used as a procedure for virus attenuation. To test if the 40F-p8 virus was attenuated *in vivo* we performed an infection experiment using the interferon receptor deficient (IFNAR$^{-/-}$) A129 strain of mice. Since these mice are unable to cope with an acute virus infection and are highly susceptible to RVFV infection (Bouloy et al., 2001; Ikegami, 2017), we thought that they might offer a much more sensitive evaluation of the hypothesized attenuation of 40F-p8.

In a first assay for infectivity, 5-month-old mice were inoculated with 10^2 pfu of each virus and monitored daily during 2 weeks for the development of signs of disease (**Supplementary Figure 1**) and survival (**Figure 2A**). In mice inoculated with the parental RVFV 56/74 first signs of disease appeared at day 3, with one animal dead, one showing ruffled fur, hunched back and strongly reduced mobility and a third one showing some ruffled fur. Both animals died on day 4. The rest (2/5) remained healthy along the experiment except for a short period of ruffled fur display, rendering a final survival rate of 40%. Conversely, animals inoculated with 40F-p8 virus showed a survival rate of 67% (4/6), with the first signs of illness appearing at day 7 (ruffled fur and watery eye in one animal) and the two only deaths at day 8. In contrast, the 56/74-p8 virus caused 100% mortality 4 days after inoculation. In this case clinical signs appeared rapidly, with two animals found dead and three moribund as early as day 3. Although these data suggest a higher virulence for 56/74-p8 than for the parental strain 56/74, these differences were not statistically significant (Mantel-Cox Log-rank test) and were not further investigated.

A second experiment was then performed with challenge doses of 10^3 and 10^4 pfu for both 40F-p8 and the parental 56/74 strain. Animals inoculated with RVFV 56/74 died within the first 4 days after infection after showing watery eye and altered mobility in the previous days (**Supplementary Figure 1**). Death rates were 100% in those inoculated with 10^3 pfu and 90% in those inoculated with 10^4 pfu, with no survivors at day 10 (**Figure 2A**). Conversely, animals inoculated with 40F-p8 virus showed higher survival rates even at the highest challenge dose, with a significant number of survivors at the end of the experiment: 5/6 (83%) in those receiving 10^3 pfu, and 4/5 (80%)

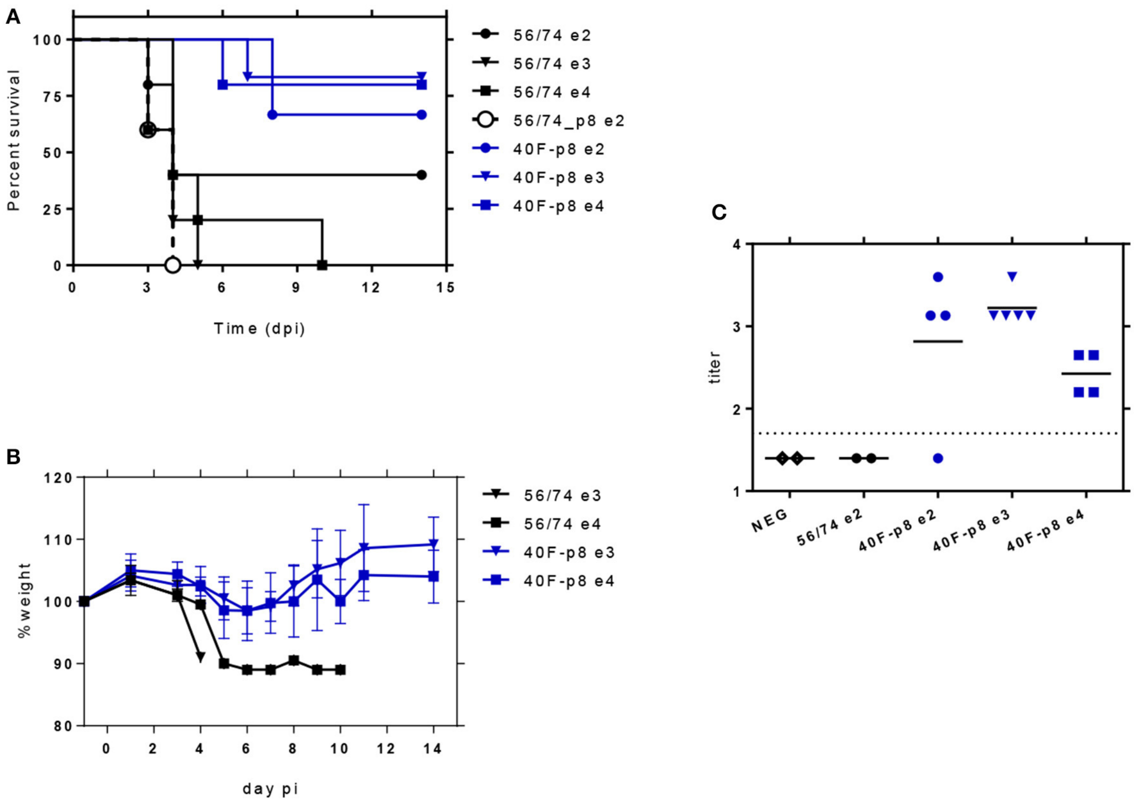

FIGURE 2 | Analysis of the *in vivo* infectivity of 40F-p8 virus in A129 mice (IFNAR$^{-/-}$). 5-6 month-old male mice (n = 5 or 6) were inoculated IP with the indicated doses of virus. Animals were monitored daily during 14 days. **(A)** Survival rates. Curve comparison was performed using the Log-Rank (Mantel-Cox) test. **(B)** Body weight change in challenged mice with the highest doses (10^3–10^4 pfu/mouse). **(C)** Detection of nucleoprotein specific antibodies by indirect ELISA. Titers are expressed as the last dilution of sera (log_{10}) giving an OD_{450} reading over 1.0. Assay cut-off threshold was set to 1.7 (dotted line, corresponding to 1/50 serum dilution). Differences were assessed using a one-way ANOVA test.

in those inoculated with 10^4 pfu (**Figure 2A**). No signs of disease were observed in any of these survivor animals except for a slight weight loss at days 3-5 pi (**Figure 2B**)

Serum samples collected at day 14 (end of the experiment) were tested by ELISA for the presence of anti-nucleoprotein N antibodies in survivors as indicative of viral replication (**Figure 2C**). In some animals within groups receiving the lowest viral dose (10^2 pfu) anti-N antibodies were undetectable, probably reflecting low or null levels of viral replication (2/2 in 56/74-inoculated mice; 1/4 in 40F-p8 inoculated mice). All animals inoculated with 10^3 and 10^4 pfu of 40F-p8, as well as three from the 10^2 group developed specific anti-N antibodies. Titers of anti-N antibodies did not show significant differences (ordinary one-way ANOVA) within groups inoculated with 40F-p8, regardless of the dose received.

Immunogenicity and Efficacy of 40F-p8 After RVFV Challenge in 129 Mice

The highly attenuated phenotype of the 40F-p8 virus displayed in immunodeficient A129 mice encouraged us to test its potential as a live attenuated vaccine in immune competent mice. With this aim, wild type 129SvEv mice were inoculated intraperitoneally (ip) with 10^4 pfu of the 40F-p8 virus, and 4 weeks later they were challenged with a lethal dose (10^4 pfu) of RVFV 56/74. After inoculation with 40F-p8 the mice did not show any sign of disease, not even significant weight variations (not shown). In serum samples collected 24 days after inoculation (pre-challenge samples), seven out of nine mice showed a strong neutralizing antibody response (**Figure 3A**). Anti-nucleoprotein N antibodies were detected in all these samples by indirect ELISA, including two samples that scored negative in our neutralization assay, although their anti-N antibody titers were slightly lower (**Figure 3D**, blue symbols). This suggested that the 40F-p8 virus replicated in all the inoculated mice at least to an extent enough to elicit an immune response. When subjected to a lethal challenge with the virulent strain 56/74, 100% of mice survived ($P < 0.001$, χ^2 14.24, df 1) until the end of the experiment (**Figures 3B,C**) without apparent clinical display, including those in which neutralizing antibody titers had not been detected. In contrast, all mice in the control group became ill and died within day 4 (**Figures 3B,C**).

Anti-N antibody titers were found increased upon virus challenge (**Figure 3D**, red symbols), suggesting a boosting effect in the primed mice. Altogether, these results show that in spite

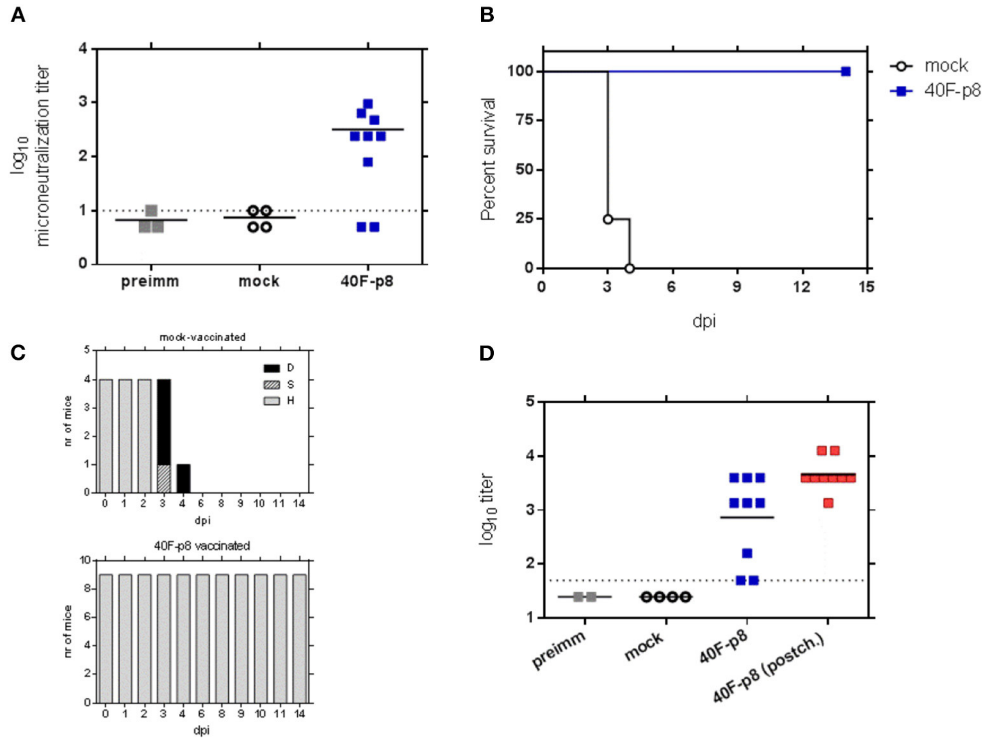

FIGURE 3 | Analysis of the immunogenicity and efficacy upon lethal RVFV challenge of 40F-p8 virus. Eleven month-old wild type 129Sv/Ev mice ($n = 9$) were inoculated IP with 10^4 pfu of 40F-p8. A group of control mice was mock-inoculated ($n = 4$). **(A)** Microneutralization assay. Serum samples were taken at day 24 (pre-challenge samples) and titrated for neutralizing antibodies. Sera were assayed in two-fold dilutions ranging from 1/10 to 1/1280. Titer was expressed as $\log_{10}$ of the highest serum dilution causing a CPE reduction of 50%. Assay cut-off was set to 1.0 (dotted line). Negative samples (rendering CPE in all wells at the first dilution assayed) were given an arbitrary value of 0.2. **(B)** Survival of 129 mice upon RVFV challenge. Differences in survival assessed with the Log-Rank (Mantel–Cox) test. **(C)** Morbidity upon challenge in vaccinated mice. The graph represents the clinical status of each mouse: D (dead): black bars; S (sick), hatched bars; H (healthy), gray bars. **(D)** Detection of anti-nucleoprotein antibodies by ELISA. Each symbol corresponds to an individual animal, except for "preimm" samples, corresponding to pools of pre-immune sera. Black/blue symbols: pre-challenge samples. Red symbols: post-challenge samples (14 dpi). Sera were assayed in three-fold dilutions ranging from 1/50-1/109350. Titers are expressed as the last dilution of sera ($\log_{10}$) giving an OD_{450} reading over 1.0. Assay cut-off threshold was set to 1.7 (dotted line, 1/50 serum dilution). For representation, negative samples were given an arbitrary value of 1.4.

of its highly attenuated phenotype the 40F-p8 virus was able to replicate in immunocompetent 129Sv/Ev mice to levels allowing the induction of protective immune responses, even when no neutralizing antibodies are detected.

Genetic Changes Found in the Selected Viruses

In order to identify genetic changes that could be related to the observed phenotypic changes, the three RNA segments of the viral genome of the viruses obtained were sequenced- The deduced amino acid sequences were then aligned and compared to that of the parental RVFV 56/74 strain. While no amino acid changes were found in the consensus sequence of the viral population recovered after eight passages without the drug, 47 nucleotide changes were found along the three RNA segments of 40F-p8 virus, leading to 24 amino acid substitutions (**Table 1**).

Most of the nucleotide changes were found in the ORFs of the corresponding RNA segments; only two changes were on 3′NCR of M segment and only one change was found in the intergenic region of segment S.

The six nucleotide changes found in the two S segment' ORFs led to only two amino acid substitutions, both in the NSs protein: V52I and P82L. Interestingly P82 belongs to the second PXXP motif involved in the nuclear localization of the NSs protein and IFN-β activation (Billecocq et al., 2004). The nucleoprotein N was the only protein of 40F-p8 virus that showed an amino acid sequence identical to that of the parental virus, with only two (silent) nucleotide substitutions.

In the coding sequence corresponding to the M segment of 40F-p8 virus a total of 15 amino acid substitutions were identified, three in the NSm gene (R26K, H108Y, E118K), eight in the Gn coding sequence [R210K (mixed), D333N, A427T, A432V, E487G, H540Y, A582T, V587I] and four in the Gc ORF (A950V, V1090I, A1116V, and R1182K). Interestingly, position R1182 (Gc) was previously involved in MP-12 virus attenuation (Ikegami et al., 2015).

The whole ORF of the L protein of the 40F-p8 virus showed seven amino acid substitutions, distributed along the entire sequence. Two changes were located in the N-term/third portion of the L-protein (M100T and H375Y); two were located in the

TABLE 1 | Total changes in the nt/aa sequence of 40F-p8 related to 56/74.

RNA segment	Protein/ region[a]	Nucleotide position changed[b]	Nucleotide (codon) changed	Amino acid position[b]	Amino acid substitution[c]
L	5′end N-term	198	GGC→GGT	60	(Gly)
		317	ATG→ACG	100	Met → Thr
		396	TTC→TTT	126	(Phe)
		1,120	CTA→TTA	368	(Leu)
		1,141	CAC→TAC	375	His → Tyr
	RdRp core	2,757	CTA→TTA	913	(His)
		2,788	GGT→AGT	924	Gly → Ser
		3,166	ATT→GTT	1050	Ile → Val
	3′end C-term	3,925	GCC→ACC	1303	Ala → Thr
		4,110	CTG→CTA	1364	(Leu)
		4,903	CTC→TTC	1629	Leu → Phe
		4,992	AAG→AAA	1658	(Lys)
		5,025	GTG→GTA	1669	(Val)
		5,178	AAG→AAA	1720	(Lys)
		5,193	AAA→AAG	1725	(Lys)
		5,229	TTC→TTT	1737	(Phe)
		6,229	GAG→AAG	2071	Glu → Lys
Total number of changes (L)			**17**		**7**
M	NSm	97	AGA→AAA	26	Arg → Lys
		342	CAC→TAC	108	His → Tyr
		372	GAG→AAA	118	Glu → Lys
		374			
	Gn	649 (mixed)[d]	AGA→AAA	210	Arg → Lys
		716	CAG→CAA	232	(Gln)
		1,017	GAT→AAT	333	Asp → Asn
		1,299	GCT→ACT	427	Ala → Thr
		1,315	GCC→GTC	432	Ala → Val
		1,337	GGT→GGA	439	(Gly)
		1,480	GAG→GGG	487	Glu → Gly
		1,638	CAC→TAC	540	His → Tyr
		1,742	CTG→CTA	574	(Leu)
		1,764	GCT→ACT	582	Ala → Thr
		1,779	GTT→ATT	587	Val →→ Ile
	Gc	2,324	AGC→AGT	768	(Ser)
		2,869	GCA→GTA	950	Ala → Val
		3,288	GTA→ATA	1090	Val → Ile
		3,359	ACC→→ACT	1113	(Thr)
		3,367	GCT→GTT	1116	Ala → Val
		3,565	AGA→AAA	1182	Arg → Lys
	3′NCR	3,821	A→G	—	—
		3,823	T→A	—	—
Total number of changes (M)			**23**		**15**
S	NSs	124	AGG→AGA	30	(Arg)
		188	GTT→ATT	52	Val → Ile
		279	CCA→CTA	82	Pro → Leu
		598	GAG→GAA	188	(Glu)
	Intergenic región	887	C→T	—	—
	NP	952	GTC→GTT	234	(Val)
		1,645	AAC→AAT	3	(Asn)
Total number of changes (S)			**7**		**2**
Total			**47**		**24**

(Continued)

[a]*Definition of regions within the RNA segments.* [b]*Amino acid and nucleotide numbering according to the sequence of RVFV SA75, accession #: DQ375428 (segment L); DQ380189 (segment M) and DQ380175 (segment S).* [c]*Amino acids are represented with the 3-letter code; when the nucleotide change did not lead to an amino acid substitution (silent mutation) the corresponding residue is written between parentheses.* [d]*Even though position 649 in the M-segment was found to show traces of the parental nucleotide (mixed) this position was computed as amino acid changed.*

C-term/third region (L1629F and E2071K), and the remaining three substitutions (G924S, I1050V and A1303T) corresponded to the central region of the protein. In particular, positions 924 and 1,050 locate within the RpRd core (region three spanning amino acid positions 895–1,206 as defined in Muller et al. (1994)), where conserved polymerase catalytic motifs A to H reside (Amroun et al., 2017; Ferron et al., 2017).

Since the viral RNA polymerase is known to be a target of favipiravir, the drug used to select the 40F-p8 virus, we evaluated the level of conservation of the mutated residues that lay within the catalytic RpRd core, in an attempt to elucidate those involved in drug resistance. With this purpose we compared the L-protein sequences corresponding to nine different RVFV strains corresponding to different genetic lineages (Bird et al., 2007) and also available sequences from 18 virus species belonging to the genus phlebovirus. Alignment ranged from amino acid position 895, the beginning of region three as described in Muller et al. (1994), to position 1,350, in order to cover also position 1,303 (**Figure 4**). The area around residue G924 (upper panel) was found to be highly conserved among all the sequences compared, as expected from its involvement on motif F (highlighted, consensus KQQHGGLREIYVMG). In particular, the residue G924 did not change in any of the sequences included. The area around position 1,050 (central panel) showed a higher level of variation among sequences. In the RVFV isolates the residue 1,050 was always isoleucine, while in the other phlebovirus species compared, other residues were found including valine (as displayed by 40F-p8). Finally, the region around A1303 displayed some degree of variation but this position was found to be extremely conserved in all the viruses included in the alignment.

As shown in **Table 1**, some of the nucleotide changes found did not lead to an amino acid substitution in the corresponding protein (residues shown in parenthesis). Even though representing a small percentage out of the total codons, these 19 silent mutations were analyzed in terms of codon usage in different expression host organisms relevant for RVF

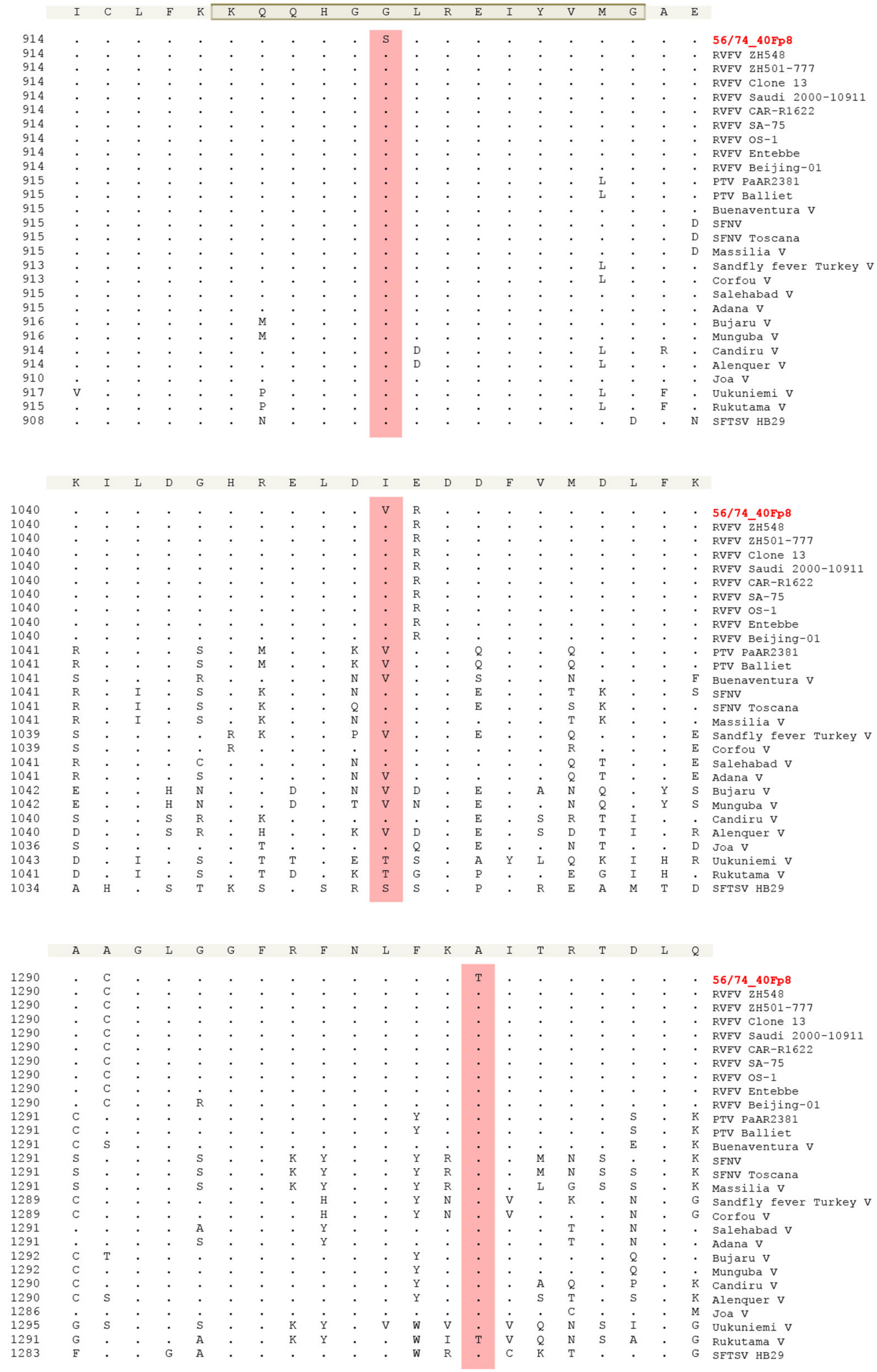

FIGURE 4 | Multiple sequence alignment of phlebovirus species RdRps. Amino acid positions shown are 914-934 (upper panel), that contains the gray-shadowed F motif (Ferron et al., 2017), 1,040–1,060 (central panel) and 1,290–1,310 (bottom panel). This numbering corresponds to the RVFVs sequences. En each panel, number in the left of each sequence indicates the amino acid position in the L protein for the corresponding virus. The alignment was generated with ClustalW using Laser gene software. GenBank accession numbers included in Materials and Methods. Residues that match the sequence of the consensus (shadowed, top of each panel) exactly are hide as ≪-≫. Positions 924 (upper), 1,050 (central) and 1,303 (bottom) where 40F-p8 virus showed amino acid substitutions are highlighted.

infection (human, sheep, and mosquito) and in mice. To analyze whether the new codons present in the virus mutant 40F-p8 corresponded to a more or less represented codon usage, the frequencies per thousand of each mutated codon were compared with those of the parental virus 56/74 (**Supplementary Table 1**). An unfavorable substitution was arbitrarily considered when ratios were ≤ 0.5 (i.e., the codon frequency in the mutant virus is half-represented in the corresponding organism related to the codon in the parental virus).

Based on this comparison we found that about half of the silent changes lead to unfavorable substitutions in both sheep and Aedes, while more similar in mice. If these silent nucleotide changes found in the 40F-p8 mutant virus exert some effect on gene expression of target organisms has not been further explored.

DISCUSSION

Rift Valley fever is an emerging zoonotic disease relevant both for animal and human health. In Africa, RVF vaccines are available for livestock although different implementation policies are followed, depending on the epidemiological or socioeconomic situation of the countries [reviewed in Dungu et al. (2018)]. Veterinary vaccines in use are both classical inactivated vaccines as well as different live attenuated vaccines (LAVs). LAVs have proven to be more effective to control the disease but their use is still limited due to the risks associated to their residual virulence in pregnant sheep (Makoschey et al., 2016). In spite of vaccination campaigns, RVF outbreaks continue to occur, and it is accepted that most human RVF cases originate from infected animals. However, a licensed vaccine for human use in endemic countries is not yet available, not even for high risk populations exposed to RVFV contagion when handling infected animals during RVF outbreaks. A live-attenuated candidate vaccine, MP12, has been tested in clinical trials in humans, providing long-term protective immunity after a single dose, with low-to-moderate side effects (Pittman et al., 2016). In 2013, the MP-12 vaccine received a conditional license for veterinary use in the U.S., but its application as human vaccine needs further improvement (reviewed in Ikegami (2017, 2019). In Europe, no RVF vaccines, either for livestock or for human use, have been licensed.

The virus characterized in this work, 40F-p8, was generated in a similar manner to MP12, i.e., by serial passages in cell culture in the presence of a mutagenic agent (Caplen et al., 1985; Ikegami, 2017; Borrego et al., 2019); and as MP12, 40F-p8 displays a number of single mutations along the three RNA-genomic segments compared to the corresponding parental virulent strain. 40F-p8 showed an extremely high attenuation *in vivo* that appears not to be related with an altered IFN-antagonistic phenotype according to the growth kinetics observed in HEK293 cells. When inoculated with a dose of 10^4 pfu, the A129 (IFNAR$^{-/-}$) mice showed a survival rate close to 80%. This was a quite remarkable finding, since this immune deficient strain of mice is highly susceptible to attenuated RVFV strains such as MP12, or even to NSm- or NSs-deletion based vaccines, with animals dying in a short period of time (Bouloy et al., 2001; Ikegami, 2017). This attenuation however did not seem to impair its immunogenicity: when inoculated in immune competent mice, 40F-p8 was able to induce a protective immune response, even in the absence of detectable neutralizing antibodies in some of the animals. This fact underscores the potential of this virus as a candidate for the development of a safe live attenuated RVF vaccine and the interest of deciphering the changes leading to the observed hyper-attenuated phenotype. Similar data on the immunogenicity of 40F-p8 was confirmed in sheep (our unpublished observations) warranting further research to evaluate the protective efficacy of 40F-p8 virus as a vaccine for ruminants.

Even though expected because of the mutagenic effect of favipiravir (Arias et al., 2014; Escribano-Romero et al., 2017; Borrego et al., 2019), the high number of changes displayed by 40F-p8 (47 nucleotide changes, 24 amino acid substitutions) strongly hinders the identification of those responsible for the observed phenotype(s), especially attenuation. As previously reported for MP12, attenuation might be achieved by a combination of several individual amino acid changes (Ikegami et al., 2015). In fact, one of the many changes displayed by 40F-p8 in the glycoproteins (R1182K) affects the same residue already identified to contribute to attenuation of the strain MP12 (R1182G) (Ikegami et al., 2015). The other 14 aa substitutions in the M ORFs, although in positions not described (to our knowledge) to have a role in attenuation are to be investigated. Besides, silent nucleotide changes leading to misrepresented codons, even though representing a very low percentage, might have some effect on gene expression (Baker et al., 2015).

Changes in other proteins are more likely to be contributing to attenuation, for instance, those involving the NSs protein, known to be the main virulent factor, and in particular the P82L change, affecting the second PXXP motif of the protein (positions 82 to 85). Experiments in cells transiently transfected with mutant proteins where proline residues were substituted by alanine showed that the mutated protein did not reach the correct nuclear localization and lost their IFN-inhibiting activity (Billecocq et al., 2004). However, in agreement with the intact growth phenotype displayed by 40F-p8 in interferon responsive HEK293 cells, our preliminary results indicate that the single P82L mutation does not impair nuclear NSs fibril-like formation (Borrego et al., 2021).

Since RNA polymerases are targets of favipiravir, the mutagenic drug that led to selection of the attenuated 40F-p8 virus, changes found in this protein were especially interesting, in particular those in the central area corresponding to the RdRp core: G924S, I1050V, and A1303T. In a structural model of L-protein, residue 924 is located within motif F in the RdRp core (Muller et al., 1994; Gerlach et al., 2015; Amroun et al., 2017; Ferron et al., 2017). Motif F is involved in the binding of the incoming rNTP (Jacome et al., 2015; Sesmero and Thorpe, 2015) and plays a key role on the interaction of favipiravir with the viral polymerase, as already described for chikungunya virus (CHIKV), coxsackievirus B3 (CVB3), and influenza virus (Delang et al., 2014; Abdelnabi et al., 2017; Goldhill et al., 2018). The location of G924 within this motif strongly suggests that substitution G924S may be responsible for the partial resistance to favipiravir of 40F-p8 virus. Its high conservation in other phleboviruses supports its role as a key position on the RdRp. The nearby residues I1050V and A1303T may be compensatory or irrelevant changes, although the fact that A1303 is also highly conserved suggests that it also may play a relevant role.

The favipiravir resistance-phenotype could be actually contributing to attenuation. Viruses selected through resistance to mutagenic drugs may show attenuation *in vivo* because of the selection of high-fidelity polymerases (Coffey et al., 2011; Cheung et al., 2014; Xie et al., 2014). Higher fidelity polymerases give raise to viral populations with reduced genetic variation, thus decreasing their chances of adaptation to successful replication in different cell types, tissues or even hosts, a feature especially important for arboviruses whose life cycles involve both mammals and insects. Of note, one of the new features of 40F-p8 virus is the impaired growth displayed in mosquito-cultured cells, although whether this impairment occurs also *in vivo* needs to be determined. Because of the aforesaid, viruses with more reliable polymerases have been proposed as a novel strategy for the development of safer live attenuated vaccines, provided that immunogenicity is maintained (Vignuzzi et al., 2008; Lauring et al., 2010; Weeks et al., 2012; Rai et al., 2017). Furthermore, a vaccine virus with a higher fidelity polymerase would provide an additional safety measure by decreasing the chance of variation during its manufacturing or (Weeks et al., 2012; Rai et al., 2017) administered. If this is the case for the virus 40F-p8 is still to be determined. Work is in progress to elucidate the contribution of the individual changes, alone or in combination, to the phenotype(s) observed and their relationship with attenuation.

In summary, in this work we have characterized an RVFV variant, 40F-p8, selected by propagation in the presence of favipiravir. 40F-p8 displays a highly attenuated phenotype in IFNAR$^{(-/-)}$ mice while retaining its immunogenicity, thus offering a promising RVF live attenuated vaccine candidate. Twenty-four amino acid substitutions were found in the viral proteins, some of them in positions potentially involved in key processes of the viral cycle. The unequivocal identification of the changes responsible for attenuation as well as the other features observed for 40F-p8 should provide remarkable information on two important aspects for RVF control. Firstly, on the interaction of the favipiravir with the viral RdRp for a better understanding of the mechanisms of action of this antiviral drug and, secondly, on the unveiling of new *in vivo* markers of virulence that would open new strategies to improve the safety of RVFV live attenuated vaccines.

MATERIALS AND METHODS

Cells, Viruses, and Infections

Vero cells (ATCC CCL-81) and HEK293T cells (ATCC CRL-3216) were grown in Dulbecco's modified Eagle's medium supplemented with 5–10% fetal calf serum (FCS), and L-glutamine (2 mM), penicillin (100 U/ml) and streptomycin (100 μg/ml), in a humid atmosphere of 5% CO2 at 37°C. C6/36 *Aedes albopictus* cells (ATCC CRL–1660) were grown in Eagle's Minimum Essential medium supplemented with 10% fetal calf serum (FCS), L-glutamine (2 mM), gentamicin (50 μg/ml), and MEM Vitamin Solution (Sigma) at 28°C. The origin of viruses used in this study has been described previously (Borrego et al., 2019). Briefly, the South African RVFV strain 56/74 (parental virus) was serially passaged in the absence or presence of 40 μM favipiravir, and virus recovered after 8 passages in the presence of the drug was named as 40F-p8. Infections were performed as described (Borrego et al., 2019).

Animal Experiments

Groups of 5-6 month-old transgenic 129Sv/Ev IFNAR$^{-/-}$ male mice (A129) or 11 month-old wild type 129Sv/Ev mice (B&K Universal) were inoculated intraperitoneally with different doses of the viruses, as indicated in the corresponding experiments. All viral inocula used were back titrated to confirm the dose administered to the mice. After viral inoculation, animals were monitored daily for weight and development of clinical signs, including ruffled fur, hunched posture, reduced activity, and conjunctivitis (eye discharge). At the indicated time-points, animals were bled through the submandibular plexus. Sera were heat-inactivated at 56°C for 30 min and kept at −20°C until use. All mice were housed in a BSL-3 room with food and water supply *ad libitum*. All experimental procedures involving animals were performed in accordance with EU guidelines (directive 2010/63/EU), and protocols approved by the Animal Care and Biosafety Ethics' Committees of INIA and Comunidad de Madrid (permit codes CEEA 2014/26, CBS 2017/15, PROEX 108/15, and PROEX192/17).

Antibody Assays

Neutralization assays were performed in 96-well culture plates following the OIE's prescribed test for RVF (*OIE Terrestrial Manual 2012. Chapter 2.1.14*). Briefly, sera were two-fold diluted from 1/10 in DMEM containing 2% fetal bovine serum, mixed with an equal volume of infectious virus containing 100 $TCID_{50}$ and incubated 30 min at 37°C. Then, a Vero cell suspension was added and plates were incubated for 4 days. Monolayers were then controlled for development of cytopathic effect (CPE), fixed and stained. Each sample was tested in four replica wells. Titer was expressed as the last dilution of serum causing CPE reduction in 50% of the wells.

For detection of antibodies against the nucleoprotein (N-protein), an in-house ELISA was performed. Briefly, ELISA plates were adsorbed with 100 ng/well of purified recombinant Trx-N protein produced in *E.coli* (Martin-Folgar et al., 2010) and diluted in carbonate buffer (pH 9.6). After blocking with 5% skimmed-milk-PBS-0.05% Tween 20, sera were tested in duplicate in serial three-fold dilutions starting at 1/50. Bound antibodies were detected with Goat Anti-mouse-IgG (H+L)-HRP Conjugated (BioRad) and bound conjugate was detected using TMB (Invitrogen/Life technologies) for 10 min, followed by one volume of stopping solution (3N H_2SO_4). Optical densities were measured at 450 nm (OD_{450}). Titers are represented as the last serum dilution ($\log_{10}$) giving an OD ≥ 1.0.

RNA Extraction, RT-PCR, and Nucleotide Sequencing

RNA was extracted from the supernatants of infected cells using the Speedtools RNA virus extraction kit (Biotools B&M Labs) according to the manufacturer's instructions. RT-PCR was performed using SuperScript IV Reverse Transcriptase (Invitrogen) and Phusion High-Fidelity DNA polymerase (Finnzymes), as directed by the manufacturers, using primers designed to amplify the S, M and L segments of the viral genome (**Supplementary Table 2**). Overlapping PCR amplicons were purified and automatically Sanger-sequenced. For 3′- and 5′-ends of the RNA segments, a RACE approach was followed using the primers described in **Supplementary Table 3**. Briefly, cDNAs from either genomic or antigenomic RNA ends were generated using Superscript IV enzyme mix. Upon RNAse H treatment, cDNAs were purified and subjected to A-tailing reaction using terminal deoxynucleotidyl transferase (TdT). After silica columm purification, PCR amplification with oligodT and RACE primers allowed sequencing of the genome ends. The Lasergene software suite (DNAstar) was used for analysis of the sequencing data.

The sequences used for multiple alignment and their database accession numbers are: RVFV ZH548 (DQ375403); RVFV ZH501 (DQ375408); RVFV Clone 13 (DQ375417); RVFV Saudi 2000-10911 (DQ375401); RVFV CAR-R1622 (DQ375423); RVFV SA-75 (DQ375428); RVFV OS-1 (DQ375398); RVFV Entebbe (DQ375429); RVFV Beijing-01 (KX611605); PTV PaAR2381 (KP272004); PTV Balliet (KR912212); Buenaventura V (KP272001); Sandfly fever Naples V(HM566172); SFNV-Toscana (NC_006319); Massilia V (EU725771.1); Sandfly Sicilian Turkey V (NC_015412.1); Corfou V (KR106177.1); Salehabad V (JX472403); Adana V (NC_029127); Bujaru V (KX611388); Munguba V (HM566164); Candiru V (NC_015374); Alenquer V (HM119401); Joa V (KX611391); Uukuniemi V (NC_005214); Rukutama V (KF892052); SFTS V HB29 (HM745930).

Statistical Analysis

Data analysis was performed using GraphPad Prism software (version 6.0).

DATA AVAILABILITY STATEMENT

The raw data supporting the conclusions of this article will be made available by the authors, without undue reservation.

ETHICS STATEMENT

The animal study was reviewed and approved by Animal Care and Biosafety Ethics' Committees of INIA and Comunidad de Madrid (permit codes CEEA 2014/26, CBS 2017/15, PROEX 108/15, and PROEX192/17).

AUTHOR CONTRIBUTIONS

AB and BB: conceptualization, methodology, formal analysis, and funding acquisition. BB: data acquisition, curation, and writing—original draft preparation. AB: writing—review and editing and project administration. All authors contributed to the article and approved the submitted version.

FUNDING

This work was supported by Grants Nos. S2013/ABI-2906 (PLATESA) and P2018/BAA-4370 (PLATESA2) from Comunidad de Madrid/FEDER and AGL2017-83326-R from Ministerio de Ciencia e Innovación. The funders had no role in the design, and writing of the report and the decision to submit the article for publication.

ACKNOWLEDGMENTS

We thank Francisco Mateos and Nuria de la Losa for excellent technical assistance. Content of this manuscript has previously appeared online in a pre-print (Borrego and Brun, 2020).

SUPPLEMENTARY MATERIAL

The Supplementary Material for this article can be found online at: https://www.frontiersin.org/articles/10.3389/fmicb.2020.621463/full#supplementary-material

REFERENCES

Abdelnabi, R., Morais, A. T. S., Leyssen, P., Imbert, I., Beaucourt, S., Blanc, H., et al.. (2017). Understanding the mechanism of the broad-spectrum antiviral activity of favipiravir (T-705): key role of the F1 motif of the viral polymerase. *J. Virol.* 91, e00487–17. doi: 10.1128/JVI.00487-17

Amroun, A., Priet, S., de Lamballerie, X., and Quérat, G. (2017). Bunyaviridae RdRps: structure, motifs, and RNA synthesis machinery. *Crit. Rev. Microbiol.* 43, 753–778. doi: 10.1080/1040841X.2017.1307805

Arias, A., Thorne, L., and Goodfellow, I. (2014). Favipiravir elicits antiviral mutagenesis during virus replication *in vivo*. *Elife* 3:e03679. doi: 10.7554/eLife.03679.021

Baker, S. F., Nogales, A., and Martinez-Sobrido, L. (2015). Downregulating viral gene expression: codon usage bias manipulation for the generation of novel influenza A virus vaccines. *Future Virol.* 10, 715–730. doi: 10.2217/fvl.15.31

Billecocq, A., Spiegel, M., Vialat, P., Kohl, A., Weber, F., Bouloy, M., et al. (2004). NSs protein of Rift Valley fever virus blocks interferon production by inhibiting host gene transcription. *J. Virol.* 78, 9798–9806. doi: 10.1128/JVI.78.18.9798-9806.2004

Bird, B. H., Albarino, C. G., Hartman, A. L., Erickson, B. R., Ksiazek, T. G., and Nichol, S. T. (2008). Rift valley fever virus lacking the NSs and NSm genes is highly attenuated, confers protective immunity from virulent virus challenge, and allows for differential identification of infected and vaccinated animals. *J Virol.* 82, 2681–2691. doi: 10.1128/JVI.02501-07

Bird, B. H., Khristova, M. L., Rollin, P. E., Ksiazek, T. G., and Nichol, S. T. (2007). Complete genome analysis of 33 ecologically and biologically diverse Rift Valley fever virus strains reveals widespread virus movement and low genetic diversity due to recent common ancestry. *J. Virol.* 81, 2805–2816. doi: 10.1128/JVI.02095-06

Borrego, B., and Brun, A. (2020). A hyper-attenuated variant of Rift Valley fever virus (RVFV) generated by a mutagenic drug (favipiravir) unveils potential virulence markers. *bioRxiv*. doi: 10.1101/2020.10.16.342170

Borrego, B., de Avila, A. I., Domingo, E., and Brun, A. (2019). Lethal mutagenesis of rift valley fever virus induced by favipiravir. *Antimicrob. Agents Chemother*. 63:e00669–19 doi: 10.1128/AAC.00669-19

Borrego, B., Moreno, S., de la Losa, N., Weber, F., and Brun, A. (2021). The change P82L in the Rift Valley fever virus NSs protein confers attenuation in mice not related with a type-I IFN antagonistic phenotype. *Preprints* 2021010439. doi: 10.20944/preprints202101.0439.v1

Boshra, H., Lorenzo, G., Busquets, N., and Brun, A. (2011). Rift valley fever: recent insights into pathogenesis and prevention. *J. Virol*. 85, 6098–6105. doi: 10.1128/JVI.02641-10

Bouloy, M., Janzen, C., Vialat, P., Khun, H., Pavlovic, J., Huerre, M., et al. (2001). Genetic evidence for an interferon-antagonistic function of rift valley fever virus nonstructural protein NSs. *J. Virol*. 75, 1371–1377. doi: 10.1128/JVI.75.3.1371-1377.2001

Briese, T., Calisher, C. H., and Higgs, S. (2013). Viruses of the family Bunyaviridae: are all available isolates reassortants? *Virology* 446, 207–216. doi: 10.1016/j.virol.2013.07.030

Caplen, H., Peters, C. J., and Bishop, D. H. (1985). Mutagen-directed attenuation of Rift Valley fever virus as a method for vaccine development. *J Gen Virol*. 66, 2271–2277. doi: 10.1099/0022-1317-66-10-2271

Cheung, P. P., Watson, S. J., Choy, K. T., Fun Sia, S., Wong, D. D., Poon, L. L., et al. (2014). Generation and characterization of influenza A viruses with altered polymerase fidelity. *Nat. Commun*. 5:4794. doi: 10.1038/ncomms5794

Coffey, L. L., Beeharry, Y., Bordería, A. V., Blanc, H., and Vignuzzi, M. (2011). Arbovirus high fidelity variant loses fitness in mosquitoes and mice. *Proc. Natl. Acad. Sci. U.S.A*. 108, 16038–16043. doi: 10.1073/pnas.1111650108

Delang, L., Segura Guerrero, N., Tas, A., Querat, G., Pastorino, B., Froeyen, M., et al. (2014). Mutations in the chikungunya virus non-structural proteins cause resistance to favipiravir (T-705), a broad-spectrum antiviral. *J. Antimicrob. Chemother*. 69, 2770–2784. doi: 10.1093/jac/dku209

Dungu, B., Lubisi, B. A., and Ikegami, T. (2018). Rift Valley fever vaccines: current and future needs. *Curr. Opin. Virol*. 29, 8–15. doi: 10.1016/j.coviro.2018.02.001

Escribano-Romero, E., Jimenez de Oya, N., Domingo, E., and Saiz, J. C. (2017). Extinction of west nile virus by favipiravir through lethal mutagenesis. *Antimicrob. Agents Chemother*. 61:e01400–17. doi: 10.1128/AAC.01400-17

Ferron, F., Weber, F., de la Torre, J. C., and Reguera, J. (2017). Transcription and replication mechanisms of bunyaviridae and arenaviridae L proteins. *Virus Res*. 234, 118–134. doi: 10.1016/j.virusres.2017.01.018

Gerlach, P., Malet, H., Cusack, S., and Reguera, J. (2015). Structural insights into bunyavirus replication and its regulation by the vRNA promoter. *Cell* 161, 1267–1279. doi: 10.1016/j.cell.2015.05.006

Goldhill, D. H., Te Velthuis, A. J. W., Fletcher, R. A., Langat, P., Zambon, M., Lackenby, A., et al. (2018). The mechanism of resistance to favipiravir in influenza. *Proc. Natl. Acad. Sci. U.S.A*. 115, 11613–11618. doi: 10.1073/pnas.1811345115

Gommet, C., Billecocq, A., Jouvion, G., Hasan, M., Zaverucha do Valle, T., Guillemot, L., et al.. (2011). Tissue tropism and target cells of NSs-deleted rift valley fever virus in live immunodeficient mice. *PLoS Negl. Trop. Dis*. 5:e1421. doi: 10.1371/journal.pntd.0001421

Ikegami, T. (2017). Rift Valley fever vaccines: an overview of the safety and efficacy of the live-attenuated MP-12 vaccine candidate. *Expert Rev. Vaccines* 16, 601–611. doi: 10.1080/14760584.2017.1321482

Ikegami, T. (2019). Candidate vaccines for human Rift Valley fever. *Expert Opin. Biol. Ther*. 19, 1333–1342. doi: 10.1080/14712598.2019.1662784

Ikegami, T., Hill, T. E., Smith, J. K., Zhang, L., Juelich, T. L., Gong, B., et al. (2015). Rift valley fever virus MP-12 vaccine is fully attenuated by a combination of partial attenuations in the S, M, and L Segments. *J. Virol*. 89, 7262–7276. doi: 10.1128/JVI.00135-15

Jacome, R., Becerra, A., Ponce de Leon, S., and Lazcano, A. (2015). Structural analysis of monomeric RNA-dependent polymerases: evolutionary and therapeutic implications. *PLoS ONE* 10:e0139001. doi: 10.1371/journal.pone.0139001

Kreher, F., Tamietti, C., Gommet, C., Guillemot, L., Ermonval, M., Failloux, A. B., et al. (2014). The Rift Valley fever accessory proteins NSm and P78/NSm-GN are distinct determinants of virus propagation in vertebrate and invertebrate hosts. *Emerg. Microbes Infect*. 3:e71. doi: 10.1038/emi.2014.71

Lauring, A. S., Jones, J. O., and Andino, R. (2010). Rationalizing the development of live attenuated virus vaccines. *Nat. Biotech*. 28, 573–579. doi: 10.1038/nbt.1635

Makoschey, B., van Kilsdonk, E., Hubers, W. R., Vrijenhoek, M. P., Smit, M., Wichgers Schreur, P. J., et al. (2016). Rift valley fever vaccine virus clone 13 is able to cross the ovine placental barrier associated with foetal infections, malformations, and stillbirths. *PLoS Negl. Trop. Dis*. 10:e0004550. doi: 10.1371/journal.pntd.0004550

Martin-Folgar, R., Lorenzo, G., Boshra, H., Iglesias, J., Mateos, F., Borrego, B., et al. (2010). Development and characterization of monoclonal antibodies against Rift Valley fever virus nucleocapsid protein generated by DNA immunization. *MAbs* 2, 275–284. doi: 10.4161/mabs.2.3.11676

Muller, R., Poch, O., Delarue, M., Bishop, D. H., and Bouloy, M. (1994). Rift valley fever virus L segment: correction of the sequence and possible functional role of newly identified regions conserved in RNA-dependent polymerases. *J Gen Virol*. 75, 1345–1352. doi: 10.1099/0022-1317-75-6-1345

Pittman, P. R., Norris, S. L., Brown, E. S., Ranadive, M. V., Schibly, B. A., Bettinger, G. E., et al. (2016). Rift Valley fever MP-12 vaccine Phase 2 clinical trial: safety, immunogenicity, and genetic characterization of virus isolates. *Vaccine* 34, 523–530. doi: 10.1016/j.vaccine.2015.11.078

Poland, J. D., Calisher, C. H., Monath, T. P., Downs, W. G., and Murphy, K. (1981). Persistence of neutralizing antibody 30-35 years after immunization with 17D yellow fever vaccine. *Bull. World Health Organ*. 59, 895–900.

Rai, D. K., Diaz-San Segundo, F., Campagnola, G., Keith, A., Schafer, E. A., Kloc, A., et al. (2017). Attenuation of foot-and-mouth disease virus by engineered viral polymerase fidelity. *J. Virol*. 91:e00081–17. doi: 10.1128/JVI.00081-17

Rolin, A. I., Berrang-Ford, L., and Kulkarni, M. A. (2013). The risk of Rift Valley fever virus introduction and establishment in the United States and European Union. *Emerg. Microbes Infect*. 2:e81. doi: 10.1038/emi.2013.81

Sabin, A. B., and Blumberg, R. W. (1947). Human infection with Rift Valley fever virus and immunity twelve years after single attack. *Proc. Soc. Exp. Biol. Med*. 64, 385–389. doi: 10.3181/00379727-64-15803

Sall, A. A., Zanotto, P. M., Sene, O. K., Zeller, H. G., Digoutte, J. P., Thiongane, Y., et al. (1999). Genetic reassortment of Rift Valley fever virus in nature. *J Virol*. 73, 8196–8200. doi: 10.1128/JVI.73.10.8196-8200.1999

Sesmero, E., and Thorpe, I. F. (2015). Using the hepatitis C virus RNA-dependent RNA polymerase as a model to understand viral polymerase structure, function and dynamics. *Viruses* 7, 3974–3994. doi: 10.3390/v7072808

Vignuzzi, M., Wendt, E., and Andino, R. (2008). Engineering attenuated virus vaccines by controlling replication fidelity. *Nat. Med*. 14, 154–161. doi: 10.1038/nm1726

Weeks, S. A., Lee, C. A., Zhao, Y., Smidansky, E. D., August, A., Arnold, J. J., et al. (2012). A Polymerase mechanism-based strategy for viral attenuation and vaccine development. *J. Biol. Chem*. 287, 31618–31622. doi: 10.1074/jbc.C112.401471

Weingartl, H. M., Zhang, S., Marszal, P., McGreevy, A., Burton, L., and Wilson, W. C. (2014). Rift Valley fever virus incorporates the 78 kDa glycoprotein into virions matured in mosquito C6/36 cells. *PLoS ONE* 9:e87385. doi: 10.1371/journal.pone.0087385

Xie, X., Wang, H., Zeng, J., Li, C., Zhou, G., Yang, D., and Yu, L. (2014). Foot-and-mouth disease virus low-fidelity polymerase mutants are attenuated. *Arch. Virol*. 159, 2641–2650. doi: 10.1007/s00705-014-2126-z

Conflict of Interest: INIA has filed a national patent application (code #202030529) for 40-FP8 based RVF vaccines.

The authors declare that the research was conducted in the absence of any commercial or financial relationships that could be construed as a potential conflict of interest.